Clemson University

College of Engineering and Science
Control and Robotics (CRB) Technical Report

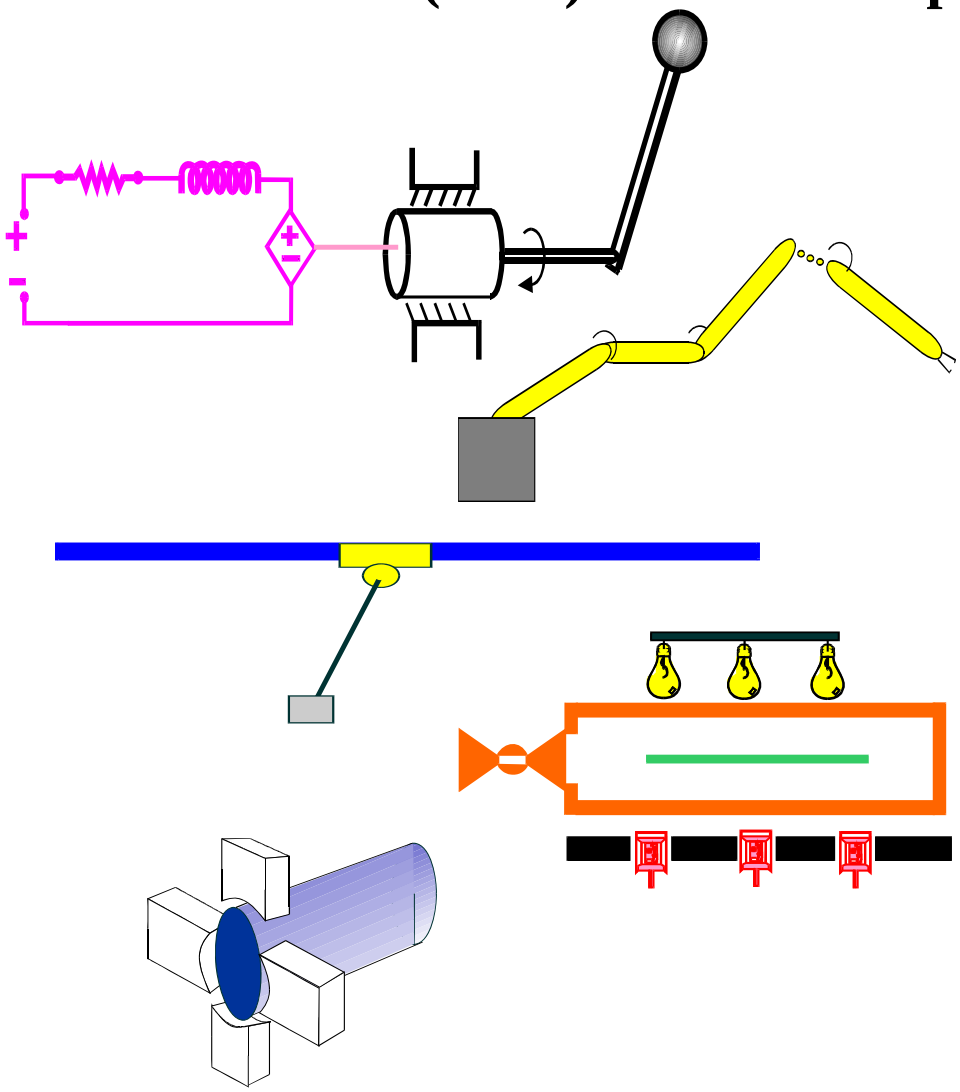

Number: CU/CRB/6/19/08/#1

Title: **Nonlinear Robust Control to Maximize Energy Capture in a Variable Speed Wind Turbine Using a Separately Excited DC Generator**

Authors: E. Iyasere, M. Salah, Dawson and J. Wagner.

Nonlinear Robust Control to Maximize Energy Capture in a Variable Speed Wind Turbine Using a Separately Excited DC Generator

E. Iyasere*, M. Salah, Ph.D., D. Dawson, Ph.D., and J. Wagner, Ph.D., P.E.

Abstract: The emergence of wind turbine systems for electric power generation can help satisfy the growing global demand. This paper proposes a control strategy to maximize the wind energy captured in a variable speed wind turbine, with a separately excited DC internal generator, at low to medium wind speeds. The proposed strategy controls the tip speed ratio, via the rotor angular speed, to an optimum point at which the efficiency constant (or power coefficient) is maximal for a given blade pitch angle. This control method allows for aerodynamic rotor power maximization without exact wind turbine model knowledge. Representative numerical results demonstrate that the wind turbine can be controlled to achieve maximum energy capture.

I. Introduction

Wind energy has evolved into an attractive energy source for electric utilities, although it is currently responsible for only one percent of the global electrical power production. The structure of wind turbines, as well as the fact that the wind energy rate is uncontrollable, compounds the problem of regulating the power capture. This engineering challenge has been alleviated by the construction of variable speed wind turbines, which are designed to regulate the power captured over a range of operating speeds. However, the efficiency of power regulation is dependent on the selected control method

Wind turbine control methods include classical techniques [1]-[3], which utilize a linearized wind turbine system model and a single measured wind turbine output for control. In [2], a PID controller compensated for wind speed fluctuations by changing the pitch angle to keep the rotor speed constant. The controller is improved by selecting gain values based on minimization of rotor speed error and the actuator duty cycle. Another common control method is full state feedback [4]-[7], which is sensitive to errors in modeling and measurements. Liebst [4] used individual blade pitch linear quadratic Gaussian (LQG) optimal control to reduce the loads on a wind turbine due to environmental factors such as shear and gravity. The dynamics of the wind turbine blade flap, lag and pitch are modeled. Knudsen et al. [5] compared PI and H_∞ controllers for regulating the pitch of a 400kW wind turbine. The H_∞ controller accounts better for turbine model uncertainties as well as error in measuring the wind speed, thus reducing pitch activity.

Fuzzy logic control [8]-[10] and neural networks [11] have been investigated to reduce the uncertainties faced by classical control methods. Prats et al. [9] presented a fuzzy logic application for enhanced energy capture in a variable speed, variable pitch wind turbine. A dynamic model was developed using torque and blade pitch fuzzy control and produced better results than linear control. Zhang et al. [10] compared PID and fuzzy logic control in the control of the rotation of the wind wheel and reverse moment of the generator in a variable speed wind turbine and concluded that fuzzy logic control produce a smoother output with less susceptibility to disturbances.

Adaptive and robust control schemes [12]-[16] have been developed to eliminate some of the problems faced in wind turbine control, such as unknown model parameters and structural uncertainties in the wind turbine model. Song et al. [13] used a model reference adaptive control scheme to force a wind turbine with a known power efficiency function, to track a desired rotor speed that maximizes the energy captured by controlling the excitation winding voltage of the generator. Iyasere et al. [16] proposed a robust control strategy to control the blade pitch angle actuator torque and generator torque in a variable speed, variable pitch wind turbine. This approach maximizes the energy capture in low to medium wind speeds without knowledge of the optimal tip speed rotor using a wind turbine model with structural uncertainties.

The control of the dynamics of the internal generator used in wind turbines has been extensively researched in [10], [13], [17]-[25]. Mihet-Popa et al. [17] described a wind turbine generator model, which is being developed to simulate the interaction between a wind turbine and the power system. The model is intended to simulate the behavior of the wind turbine using induction generators. Morimoto et al [18] proposed an output power maximization control strategy for a wind generation system. A permanent magnet synchronous generator (PMSG) is used as a variable speed generator in the proposed system, with the generator torque controlled according to the generator speed using maximum power point tracking (MPPT) control. Additionally, the control objective is achieved without mechanical sensors such as wind velocity and position measurements. Leithead and Connor [19] described the control of a variable speed wind turbine with an induction generator. The system to be controlled is assumed to be multivariate with the desired generator torque and pitch demand as inputs and the generator torque and speed as outputs. In [24], a nonlinear adaptive based controller is designed for the field weakening area of a separately excited DC motor.

*To whom all correspondence should be addressed
E. Iyasere, D. M. Dawson and J. Wagner are with the College of Engineering and Science, Clemson University, Clemson, SC 29634-0915 (e-mail: oiyaser@clemson.edu; darren.dawson@ces.clemson.edu; jwagner@clemson.edu).
M. Salah is with the Department of Mechatronics Engineering, Hashemite University, Zarqa, Jordan (email: msalah@hu.edu.jo)

The control objective was to force the mechanical speed and back EMF to track a linear reference model in the presence of parameter uncertainties by controlling the armature and field voltages.

In this study, a control strategy is developed to regulate the rotor speed of a variable speed wind turbine system with a separately excited DC generator. The control objective is to maximize the energy captured by the wind turbine for low to medium air speeds by tracking a desired rotor speed in the presence of system nonlinearities and structural uncertainty. Additionally, the maximization of the energy captured is achieved without the knowledge of the relationship that governs the power capture efficiency of the wind turbine. Instead, an optimization algorithm is developed to seek the unknown optimal rotor speed that maximizes the energy captured (via the aerodynamic rotor power), at a given blade pitch angle, while ensuring that the resulting trajectory is sufficiently differentiable. The disadvantage of not explicitly knowing the rotor speed *a priori* is countered by the fact that the optimal rotor speed will change as the wind speed changes which may be accommodated by the optimization algorithm. A robust controller is designed and proven to yield a globally uniformly ultimately bounded (GUUB) stable closed loop system through Lyapunov-based analysis.

The paper is organized as follows. In Section II, a wind turbine dynamic model will be presented. In Section III, a robust tracking controller is introduced along with the error system dynamics. The stability analysis is presented in Section IV. In Section V, the system nonlinearities have been estimated. The reference trajectory generation is discussed in Section VI, followed by numerical simulation results in Section VII. Concluding remarks are presented in Section VIII.

II. Dynamic Model Development

The wind turbine model consists of a wind rotor, low-speed shaft, gear box, high-speed shaft and a separately excited DC generator. The block diagram is shown in Fig. 1. The aerodynamic rotor power is dependent on the available wind power and the power coefficient. The power coefficient is a function of two variables: the tip-speed ratio (TSR) and the blade pitch angle. The rotor power of the wind turbine, $P_{\text{aero}}(t) \in \mathbb{R}$, can be defined as

$$P_{\text{aero}} = \frac{1}{2} C_p(\lambda, \beta) \rho_a A v^3 \tag{1}$$

where $\rho_a \in \mathbb{R}$ is the air density, $A \in \mathbb{R}$ is the rotor swept area, $v(t) \in \mathbb{R}$ is the wind speed, $C_p(\cdot) \in \mathbb{R}$ denotes the power coefficient of the wind turbine, which is assumed to be unknown, $\lambda(t) \in \mathbb{R}$ is the tip-speed ratio, and $\beta \in \mathbb{R}$ represents the blade pitch angle. The tip-speed ratio, $\lambda(t)$, is defined as

$$\lambda = \frac{\omega R}{v} \tag{2}$$

where $\omega(t) \in \mathbb{R}$ is the rotor angular speed and $R \in \mathbb{R}$ is the rotor radius. From (1) and (2), an optimal rotor speed, ω^*, exists for a particular wind speed, $v(t)$, and blade pitch angle, β, at which the power capture efficiency is maximum, with $C_p^{\max} = C_p(\lambda^*, \beta)$ and $\lambda^* = \dfrac{\omega^* R}{v}$.

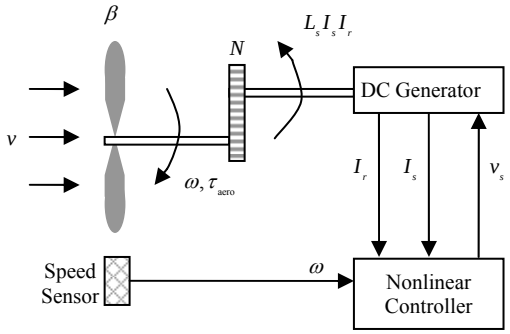

Fig. 1: Block diagram of wind turbine

The rotor power, $P_{\text{aero}}(t)$, can also be written as

$$P_{\text{aero}} = \tau_{\text{aero}} \omega \tag{3}$$

where $\tau_{\text{aero}}(t) \in \mathbb{R}$ is the aerodynamic torque applied to the rotor by the wind. An expression for $\tau_{\text{aero}}(t)$ can be derived from (1)-(3) as

$$\tau_{\text{aero}} = \frac{1}{2} \rho_a A R \frac{C_p(\lambda, \beta)}{\lambda} v^2 \tag{4}$$

Remark 1: In (1), it is assumed that $C_p(\cdot)$ is unknown which implies that $\tau_{\text{aero}}(\cdot)$ is unmeasurable.

The wind turbine model structure consists of a mechanical subsystem describing the rotor dynamics of the variable speed wind turbine and generator stator coil current electrical subsystem [10], [15], [25]-[26]. The mechanical subsystem dynamics are given by

$$J\dot{\omega} + B\omega + f(\omega, v) = -NK_B L_s I_s I_r \tag{5}$$

where $J \in \mathbb{R}^+$ denotes the scaled sum of the rotor and generator inertias, $B \in \mathbb{R}^+$ contains the scaled mechanical damping coefficients describing the rotor and generator, $f(\omega, v) \triangleq -\tau_{\text{aero}}(t)$ represents the system nonlinearities, $N \in \mathbb{R}^+$ denotes the gearbox ratio of the high speed rotor to the low speed rotor, $K_B \in \mathbb{R}^+$ is the constant back-emf parameter, $I_r(t) \in \mathbb{R}$ and $I_s(t) \in \mathbb{R}$ describe the rotor and stator currents, respectively, and $L_s \in \mathbb{R}^+$ is the constant inductance of the stator coil. The stator coil current, $I_s(t)$, is governed by the following electrical subsystem

$$L_s \dot{I}_s = v_s - R_s I_s \tag{6}$$

where $v_s(t)$ is the stator (control) voltage and $R_s \in \mathbb{R}^+$ represents the constant resistance in the stator electrical subsystem.

To facilitate the control development process, the following model characteristics are assumed:

Assumption 1: The parameters J, R, A, ρ_a, L_s, R_s, K_B, β and N are known constants.

Assumption 2: $\omega(t)$, $\dot{\omega}(t)$, $I_s(t)$, $I_r(t)$ and $v(t)$ are measurable.

Assumption 3: The rotor coil subsystem is connected to the electrical grid and is current regulated such that $I_r(t)$ is constant and non-zero.

Assumption 4: $v(t)$ is constant or slowly time varying (i.e. $\dot{v} \cong 0$).

Assumption 5: $v(t), \dot{v}(t), \ddot{v}(t)$ are bounded.

Assumption 6: $f(\omega, v)$ is unknown because $\tau_{\text{aero}}(t)$ is unknown.

Assumption 7: The variables, $f(\omega, v)$, $\dot{f}(\omega, \dot{\omega}, v, \dot{v})$, $\ddot{f}(\omega, \dot{\omega}, \ddot{\omega}, v, \dot{v}, \ddot{v})$ are bounded such that $f(\cdot)$, $\dot{f}(\cdot)$, $\ddot{f}(\cdot) \in \mathcal{L}_\infty$ if $\omega(t), \dot{\omega}(t), \ddot{\omega}(t) \in \mathcal{L}_\infty$.

Remark 2: $|f(\omega, v)|$ can be upper bounded by a known function such that $|f(\omega, v)| \le \rho(\omega)$ where $\rho(\omega)$ is continuously differentiable.

III. Error System Development

The control objective is to maximize the aerodynamic rotor power of the wind turbine, $P_{\text{aero}}(t)$, while tracking a developed desired rotor speed $\omega_d(t) \in \mathbb{R}$ such that $\omega \to \omega_d$ as $t \to \infty$. To quantify this objective, tracking errors denoted by $e(t), \eta_s(t) \in \mathbb{R}$ are defined as

$$e \triangleq \omega_d - \omega \; ; \; \eta_s \triangleq I_s - I_d \tag{7}$$

where $I_d(t) \in \mathbb{R}$ is the subsequently designed desired stator current.

Remark 3: $\omega_d(t)$ is planned online using a numerical-based optimization algorithm to maximize the rotor power $P_{\text{aero}}(t)$ at a given pitch angle, β, and wind velocity, $v(t)$, such that $\omega_d(t) \to \omega^*$, hence $P_{\text{aero}}(t) \to P_{\max}$ where $P_{\max} \triangleq \frac{1}{2} C_p^{\max} \rho A v^3$ and the optimal speed, ω^*, is the result of the optimum seeking algorithm after convergence. The variable $\omega_d(t)$ is designed such that $\omega_d(t), \dot{\omega}_d(t), \ddot{\omega}_d(t) \in \mathcal{L}_\infty$.

From the definition of the tracking errors in (7) and system dynamics in (5) and (6), an open loop error system is developed as follows

$$J\dot{e} = J\dot{\omega}_d + B\omega + f(\omega, v) + NK_B L_s I_r \eta_s + NK_B L_s I_r I_d \tag{8}$$

$$L_s \dot{\eta}_s = -R_s I_s + v_s - L_s \dot{I}_d \tag{9}$$

Based on the subsequent stability analysis in the Section IV and the structure of the open loop error system in (8) and (9), the desired stator current, $I_d(t)$, and the control voltage, $v_s(t)$, are designed as follows

$$I_d = \frac{1}{NK_B L_s I_r}\left(-ke - \frac{\rho^2(\omega) e}{\varepsilon} - J\dot{\omega}_d - B\omega + \hat{f}_s\right) \tag{10}$$

$$v_s = -NK_B L_s I_r e - k_s \eta_s + R_s I_s + L_s \dot{I}_d \tag{11}$$

where $\hat{f}_s(\cdot) \triangleq \frac{1}{\tau s + 1} \text{sat}\left\{\hat{f}(\cdot)\right\}$, $\hat{f}(\cdot)$ is an estimate of $f(\cdot)$ which is designed later in Section V, s is the Laplace variable, $k, k_s \in \mathbb{R}^+$ are control gains, $\varepsilon, \tau \in \mathbb{R}^+$ are small constants and $\rho(\omega)$ is defined in Remark 2.

Remark 4: $\hat{f}_s(\cdot), \dot{\hat{f}}_s(\cdot) \in \mathcal{L}_\infty$ since $\text{sat}\{\cdot\} \in \mathcal{L}_\infty$ and $\frac{1}{\tau s + 1}$ is a proper bounded filter. Thus, it may be assumed that $\left|\hat{f}_s(\cdot)\right| \le \rho_s$ where $\rho_s \in \mathbb{R}^+$.

Substituting (10) and (11) into the open-loop dynamics of (8) and (9), results in the following closed-loop error system

$$J\dot{e} = -ke - \frac{\rho^2 e}{\varepsilon} + f + \hat{f}_s + NK_B L_s \eta_s I_r \tag{12}$$

$$L_s \dot{\eta}_s = -NK_B L_s I_r e - k_s \eta_s \tag{13}$$

IV. Stability Analysis

Theorem 1: Given the closed loop error system in (12) and (13), all signals are bounded and the tracking error signals given in (7) are globally uniformly ultimately bounded (GUUB).

Proof: Refer to Appendix A.

V. Design of Nonlinearity Estimate $\hat{f}(\cdot)$

The control objective is to maximize the aerodynamic rotor power captured by a variable speed wind turbine with structurally uncertain system nonlinearities by controlling the rotor speed, $\omega(t)$. This model property requires that the system nonlinearities, $f(\cdot)$, be estimated. This estimate of $f(\cdot)$, denoted by $\hat{f}(\cdot)$, is developed for two reasons:

I. $\hat{f}(\cdot)$ is used as a feed-forward term in the control design through $\hat{f}_s(\cdot)$.

II. From Remark 1 and (3), it can be concluded that $P_{\text{aero}}(t)$ is unmeasurable. An estimate of the captured power, $\hat{P}_{\text{aero}}(t)$, can be realized where $\hat{P}_{\text{aero}}(t) = -\hat{f}(t)\omega(t)$.

In the robust control design, it has been proven that $f(\cdot), \dot{f}(\cdot), \ddot{f}(\cdot) \in \mathcal{L}_\infty$. Now consider the two systems

$$\begin{aligned} J\dot{\omega} &= -NK_B L_s I_r I_s - f(\cdot) - B\omega \\ J\dot{\hat{\omega}} &= -NK_B L_s I_r I_s - \hat{f}(\cdot) - B\hat{\omega} \end{aligned} \tag{14}$$

where $\hat{\omega}(t) \in \mathbb{R}$ denotes the estimate of the rotor speed, $\omega(t)$, and $\hat{f}(\cdot)$ is the estimate of $f(\cdot)$ that is determined from the subsequently designed estimator.

The objective of the estimator is to track the system nonlinearities $f(\cdot)$ such that $\hat{f}(\cdot) \to f(\cdot)$ as $t \to \infty$. To quantify this objective, the observer errors, $\tilde{\omega}(t), \tilde{f}(t) \in \mathbb{R}$ are defined as

$$\tilde{\omega} \triangleq \hat{\omega} - \omega, \quad \tilde{f} \triangleq \hat{f} - f \tag{15}$$

The filtered observer error, denoted by $r(t) \in \mathbb{R}$, is defined to facilitate the subsequent design and analysis as

$$r \triangleq \dot{\tilde{\omega}} + \left(\Delta + \frac{B}{J}\right)\tilde{\omega} \tag{16}$$

where $\Delta \in \mathbb{R}^+$ is a constant. After taking the time derivative of (16) and pre-multiplying by M, it may be shown that

$$J\dot{r} = J\ddot{\tilde{\omega}} + (\Delta J + B)\dot{\tilde{\omega}} = -\dot{\tilde{f}} + \dot{f} + \Phi - \tilde{\omega} \tag{17}$$

where $\Phi = \Delta J\dot{\tilde{\omega}} + \tilde{\omega}$.

Remark 5: Φ can be upper bound such that $\Phi \le \rho_{\text{N}} \|\bar{z}\|$ where $\bar{z}(t) = \left[\tilde{\omega}(t), r(t)\right]^{\text{T}}$ and $\rho_{\text{N}} \in \mathbb{R}^+$ is a constant.

Based on the structure of (17), as well as the subsequent stability analysis, a continuous estimator law is proposed to achieve the stated estimator objectives with

$$\dot{\hat{f}} = \left(k_f + \Delta + \frac{B}{J}\right) r + \rho_0 \operatorname{sgn}(\tilde{\omega}) \tag{18}$$

where $k_f, \rho_0 \in \mathbb{R}^+$ are control gains.

Before presenting the stability analysis, the following lemma will be introduced and later invoked.

Lemma 1: Let the auxiliary function $L(t) \in \mathbb{R}$ be defined as

$$L \triangleq r\left(\dot{f} - \rho_0 \operatorname{sgn}(\tilde{\omega})\right) \tag{19}$$

If the control gain ρ_0 is selected to satisfy the sufficient condition $\rho_0 > \left|\dot{f}\right| + \frac{\left|\ddot{f}(\cdot)\right|}{\Lambda}$, then $\int_{t_0}^{t} L(\tau)\, d\tau \le \zeta$ where $\Lambda \triangleq \Delta + \frac{B}{J}$ and $\zeta \in \mathbb{R}^+$ is

$$\zeta \triangleq \rho_o \left|\tilde{\omega}(t_0)\right| - \tilde{\omega}(t_0)\, \dot{f}(t_0) \tag{20}$$

Proof: See [27] for a similar proof.

Theorem 2: The estimator law of (18) ensures that all system signals are bounded and asymptotic tracking in the sense that $\tilde{\omega}(t), \dot{\tilde{\omega}}(t), r(t) \to 0$ as $t \to \infty$ can be obtained.

Proof: See [27] for a similar proof.

From (14), the following relationship can be obtained

$$J\dot{\tilde{\omega}} = f - \hat{f} - B\tilde{\omega} = -\tilde{f} - B\tilde{\omega} \tag{21}$$

From (21), it is clear that $\lim_{t\to\infty} \tilde{\omega}(t), \dot{\tilde{\omega}}(t) = 0$, hence $\tilde{f}(t) \to 0$ as $t \to \infty$.

VI. Trajectory Generator

In Remark 2, it is assumed that a desired trajectory $\omega_d(t)$ can be designed such that $\omega_d \in c^2$, $\omega_d(t), \dot{\omega}_d(t), \ddot{\omega}_d(t), \in \mathcal{L}_\infty$ and $\omega_d \to \omega^*$ where ω^* is the unknown rotor speed that maximizes the aerodynamic rotor power, $P_{\text{aero}}(t)$, for a particular wind speed, $v(t)$, and blade pitch angle, β, via the tip speed ratio, λ. As stated in the previous section, $P_{\text{aero}}(t)$ is unmeasurable. Instead, the estimated captured power, $\hat{P}_{\text{aero}}$, can be used as the cost function to be optimized. The optimum seeking algorithm selected is the Successive Quadratic Estimator (SQE). The advantage of using this algorithm over conventional methods, such as the Golden Section Search, is that no initial cost function values or bounds on the functional values are required. This method approximates the unimodal cost function, $\hat{P}_{\text{aero}}(\omega)$, as a quadratic function over a local bound and successively uses this property to predict the location of ω^*, the optimum rotor speed [28].

To ensure that $\omega_d(t), \dot{\omega}_d(t), \ddot{\omega}_d(t), \in \mathcal{L}_\infty$, a filter based form of the SQE method is used, wherein at each iteration, $\omega_d[n]$ is passed through a set of third order stable and proper low pass filters to generate continuous bounded signals for $\omega_d(t), \dot{\omega}_d(t), \ddot{\omega}_d(t)$. The filters shown in (22)-(24) are used in this study, where $\zeta_1, \zeta_2, \zeta_3, \zeta_4 \in \mathbb{R}^+$ are filter constants and s is the Laplace variable. The optimization algorithm waits until certain error thresholds are met before making the next guess (*i.e.*, if $\left|\omega_d(t) - \omega_d[n]\right| \le \bar{e}_1$, $\left|\tilde{f}(\cdot)\right| \le \bar{e}_2$ and $\left|\omega(t) - \omega_d(t)\right| \le \bar{e}_3$ then $n = n+1$) where $e_1, e_2, e_3 \in \mathbb{R}^+$ are constants and $n \in \mathbb{Z}^+$

$$\omega_d(t) = \frac{\zeta_1}{s^3 + \zeta_2 s^2 + \zeta_3 s^3 + \zeta_4}\, \omega_d[n] \tag{22}$$

$$\dot{\omega}_d(t) = \frac{\zeta_1 s}{s^3 + \zeta_2 s^2 + \zeta_3 s^3 + \zeta_4}\omega_d[n] \qquad (23)$$

$$\ddot{\omega}_d(t) = \frac{\zeta_1 s^2}{s^3 + \zeta_2 s^2 + \zeta_3 s^3 + \zeta_4}\omega_d[n] \qquad (24)$$

VII. Simulation Results

A numerical case study is presented in this section to demonstrate the performance of the controller introduced in Section III and the numerical-based optimum seeking reference trajectory generator. The plant model in (5) was assumed to correspond to a small wind turbine, possessing the following system nonlinearity

$$f(\cdot) = -\frac{1}{2}\rho A \frac{C_p(\lambda)}{\omega} v^3 \qquad (25)$$

The simulation parameters are listed in Appendix B. The desired and actual rotor angular speeds, $\omega_d(t)$ and $\omega(t)$, respectively, are shown in Fig. 2. It is clear that $\omega(t)$ successfully tracks $\omega_d(t)$. The power coefficient function, $C_p(\lambda)$, for the wind turbine, illustrated in Fig. 3a, was obtained using blade-element momentum theory [29]. It may be observed that $C_p^{\max} = 0.4494$ occurs when $\lambda^* = 7$ which corresponds to $\omega^* = 3.5$. The actual power efficiency measure, $C_p(t)$, shown in Fig. 3b, converges to $C_p = 0.4493$ which is equivalent to $\omega_d = 3.5506$ in Fig. 2. From Figs. 2 and 3, it can be concluded that $\omega(t) \to \omega_d(t)$ and $\omega_d(t) \to \omega^*$, thus $\omega(t) \to \omega^*$, which fulfills the stated control objective. Additionally, the control voltage, $v_s(t)$, stator current, $I_s(t)$, and stator current error, $\eta_s(t)$, shown in Figs. 4 and 5, confirm that the closed loop error system is globally uniformly ultimately bounded and all signals are bounded. Note that the control voltage, $v_s(t)$, is restricted to its rated value of $\pm 240\text{V}$, to simulate realistic stator behavior.

Overall, the simulation results demonstrate that the proposed control strategy has good performance and shows a robust response to structural uncertainties.

VIII. Conclusions

A nonlinear controller has been developed for a variable speed wind turbine system to optimize the energy captured by the wind turbine for a particular blade pitch angle. A desired rotor speed trajectory generator is provided that seeks the unknown optimal set-point while ensuring the trajectory remains bounded and sufficiently differentiable. To track the desired trajectory, a robust controller is developed, which is proven to yield a globally uniformly ultimately bounded stable closed-loop system via Lyapunov-based analysis. Simulation results demonstrate the satisfactory performance of the robust controller and the numerical-based optimum seeking algorithm. The next task in the project is the implementation of the control strategy on a validated wind turbine model.

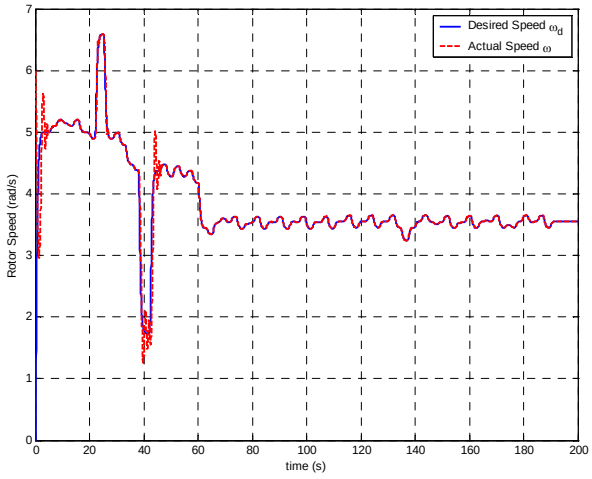

Fig. 2: Desired rotor speed $\omega_d(t)$ and actual rotor speed $\omega(t)$

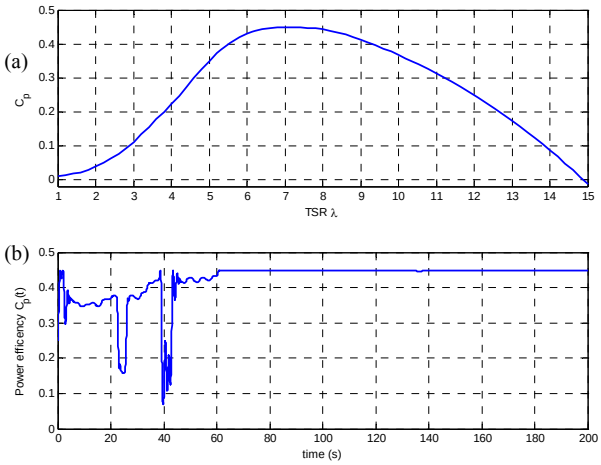

Fig. 3: (a) Power efficiency curve for simulated wind turbine, and (b) maximum rotor power coefficient $C_p(t)$ resulting from numerical optimization algorithm

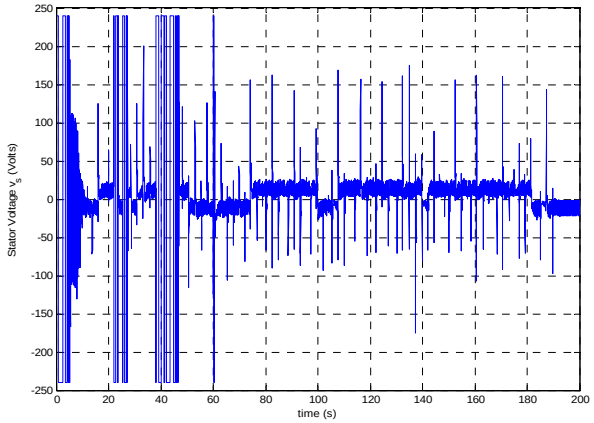

Fig. 4: Stator control voltage $v_s(t)$ versus time

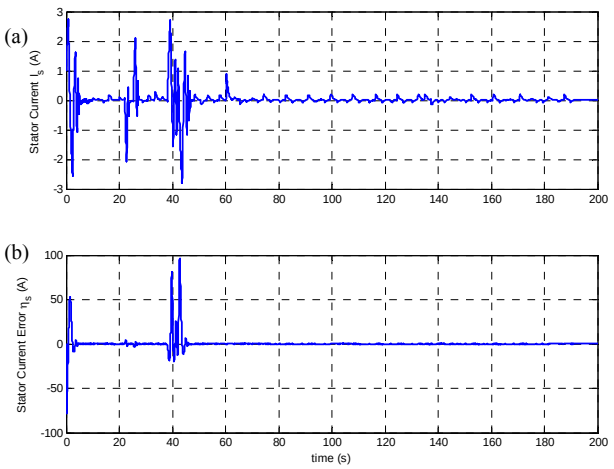

Fig. 5: Stator coil subsystem with (a) stator coil current $I_s(t)$, and (b) stator coil current error $\eta_{I_s}(t)$

REFERENCES

[1] M. Hand and M. Balas, "Non-linear and linear model based controller design for variable-speed wind turbines," presented at the 3rd ASME/JSME Joint Fluids Engineering Conf., San Francisco, CA, 1999.

[2] B. Malinga, J. Sneckenberger, and J. Feliachi, "Modeling and control of a wind turbine as a distributed resource," in *Proc. 35th Southeastern Symp. Syst. Theory*, Morgantown, WV, 2003, pp.. 108-112.

[3] J. Svensson and E. Ulen, "The control system of WTS-3 instrumentation and testing," in *Proc. 4th Int. Symp. Wind Energy Systems*, Stockholm, Sweden, 1982, pp. 195-215.

[4] B. Liebst, "Pitch control system for large-scale wind turbines," *J. of Energy*, vol. 7, no. 2, pp. 182-192, 1983.

[5] T. Knudsen, P. Andersen, and S. Tiffner-Clausen, "Comparing PI and robust control pitch controllers on a 400KW wind turbine by full scale tests," Department of Control Engineering, Aalborg University, Aalborg, Denmark, Tech. Rep. R-97-4174, 1997.

[6] S. Mattson, ''Modeling and control of large horizontal axis wind power plants,'' Ph.D. Thesis, Lund Institute of Technology, Lund, Sweden, 1984.

[7] K. Stol and M. Balas, "Full-state feedback control of a variable-speed wind turbine: A comparison of periodic and constant Gains", *J. of Solar Energy Eng.*, vol. 123, no. 4, pp. 319-326, 2001.

[8] R. Chedid, S. Karaki, and C. El-Chamali, "Adaptive fuzzy control for wind-diesel weak power systems," *IEEE Trans. Energy Conversion*, vol. 15, no. 1, pp. 71-78, March 2000.

[9] M. Prats, J. Carrasco, E. Galvan, J. Sanchez, L.Franquelo and C. Batista, "Improving transition between power optimization and power limitation of variable speed, variable pitch wind turbines using fuzzy control techniques," *Proc. IECON 2000*, Nagoya, Japan, 2000, vol. 3, pp. 1497-1502.

[10] X. Zhang, W. Wang and Y. Liu, "Fuzzy control of variable speed wind turbine", in *Proc. 6th World Congress on Intelligent Control and Automation*, Dalian, China, 2006, pp. 3872-3876.

[11] F. Kanellos and N. Hatziargyriou, "A new control scheme for variable speed wind turbines using neural networks," in *Proc. IEEE Power Eng. Soc. Trans. Distrib. Conf.*, New York, NY, 2002, pp. 360-365.

[12] J. Freeman and M. Balas, "An investigation of variable speed horizontal-axis wind turbines using direct model-reference adaptive control," in *Proc. 18th ASME Wind Energy Symp.*, Reno, NV, 1999, pp. 66-76.

[13] Y. Song, B. Dhinakaran, and X. Bao, "Variable speed control of wind turbines using nonlinear and adaptive algorithms," *J. Wind Eng. Ind. Aerodyn.*, vol. 85, no. 3, pp. 293-308, Apr. 2000.

[14] K. Johnson, L. Fingersh, M. Balas, and L. Pao, "Methods for increasing region 2 power capture on a variable-speed wind turbine", *J. Solar Energy Eng.*, vol. 126, no. 4, pp. 1092-1100, 2004.

[15] K. Johnson, L. Pao, M. Balas, and L. Fingersh, "Control of variable-speed wind turbines: Standard and adaptive techniques for maximizing energy capture", *IEEE Control Syst. Mag.*, vol. 26, no. 3, pp. 70-81, June 2006.

[16] E. Iyasere, M. Salah, D. Dawson and J. Wagner, "Nonlinear robust control to maximize energy capture in a variable speed wind turbine", *Proc. of the American Control Conference*, Seattle, Washington, 2008.

[17] L. Mihet-Popa, F. Blaabjerg, and I. Boldea, "Wind turbine generator modeling and simulation where rotational speed is the controlled variable," *IEEE Trans. Ind. Applications*, vol.40, no. 1, pp. 3-10, Jan. 2004.

[18] S. Morimoto, T. Nakamura, and Y. Takeda, "Power maximization control of variable-speed wind generation system using permanent magnet synchronous generator," *Trans. Inst. Elec. Eng. of Japan, Part B*, vol. 123-B, no. 12, pp. 1573-1579, Dec. 2003.

[19] W. E. Leithead and B. Connor, "Control of a variable speed wind turbine with induction generator," in *Int. Conf. on Control*, Coventry, UK, 1994, pp. 1215-1220.

[20] J. Ekanayake, L. Holdsworth and N. Jenkins, "Control of DFIG wind turbines," in *Proc. Inst. Elec. Eng., Power Eng.*, vol. 17, no. 1, pp. 28-32, 2003.

[21] M. G. Kanabar, C. V. Dobariya, and S. A. Khaparde, "Rotor speed stability analysis of constant speed wind turbine generators," in *Int. Conf. on Power Electronics, Drives and Energy Systems*, 2006, pp. 1-5.

[22] S. Tsiolis, O. Carlson, E. Uleín, and A. Bjoïrck, "Stall control with a variable speed wind turbine and an induction generator" in *Proc. of the Euro. Comm. Wind Energy Conf.*, Travemuende, Germany, 1993, pp. 816-819.

[23] M.Y. Uctag, I. Eskandarzadeh and H. Ince, "Modelling and output power optimisation of a wind turbine driven double output induction generator," in *IEE Proc.-Electr. Power Appl.*, vol. 141, no. 2, pp. 33-38, 1994.

[24] J. Zhou, Y. Wang, and R. Zhou, "Adaptive backstepping control of Separately Excited DC Motor with Uncertainties," in *IEE Proc. Elect. Power Appl.*, vol. 149, 2002, pp. 165–172.

[25] L Dodson, K Busawon, and M Jovanovic, "Estimation of the power coefficient in a wind conversion system," in *Proc. IEEE Conf. on Decision and Control*, Seville, Spain, 2005, vol. 1, pp. 3450-3455

[26] D. Dawson, J. Hu, and T.C. Burg, *Nonlinear Control of Electric Machinery*, New York, NY: Marcel Dekker, 1998, pp. 319-342.

[27] A. Behal J. Chen, D. M. Dawson, and X. Zhang, "A Novel path planning and control framework for passive resistance therapy with a robot manipulator," in *Proc. IEEE Conf. on Decision and Control*, Paradise Island, Bahamas, 2004, pp. 5374-5379.

[28] G. Reklaitis, A. Ravindran, and K. Ragsdell, *Engineering Optimization*, Hoboken, NJ: John Wiley & Sons, 1983, pp. 41-130.

[29] NWTC Design Codes (WT_Perf by Marshall Buhl), http://wind.nrel.gov/designcodes/simulators/wtperf/, Aug. 1, 2007.

APPENDIX

A. *Proof of Theorem 1*

A non-negative function, denoted by $V(t) \in \mathbb{R}^+$, is defined as

$$V = \frac{1}{2} J e^2 + \frac{1}{2} L_s \eta_s^2 \tag{26}$$

Taking the time derivative of (26), and substituting (12) and (13), results in

$$\dot{V} = e\left[-ke - \frac{\rho^2 e}{\varepsilon} + f + \hat{f}_s + NK_B L_s I_r \eta_s\right] + \eta_s\left[-NK_B L_s I_r e - k_s \eta_s\right] \tag{27}$$

$$\dot{V} = -ke^2 - \frac{\rho^2 e^2}{\varepsilon} - k_s \eta_s^2 + ef + e\hat{f}_s \tag{28}$$

From (28), using Remarks 2 and 4, the function $\dot{V}(t)$ can be upper bound as follows

$$\dot{V} \le -ke^2 - k_s \eta_s^2 + \rho|e| - \frac{\rho^2 e^2}{\varepsilon} + |e|\rho_s \tag{29}$$

If $k = k_1 + k_2$ with $k_1, k_2 \in \mathbb{R}^+$, then

$$\dot{V} \le -k_1 e^2 - k_s \eta_s^2 \underbrace{-k_2 e^2 + |e|\rho_s}_{\frac{\rho_s^2}{4k_2} - \left(\sqrt{k_2}e - \frac{\rho_s}{2\sqrt{k_2}}\right)^2} + \rho|e|\left(1 - \frac{\rho|e|}{\varepsilon}\right) \tag{30}$$

From (30), $\dot{V}(t)$ can be upper bound as follows

$$\dot{V} \le -k_1 e^2 - k_s \eta_s^2 + \rho|e|\left[1 - \frac{\rho|e|}{\varepsilon}\right] + \frac{\rho_s^2}{4k_2} \tag{31}$$

$$\dot{V} \le -\gamma \|z\|^2 + \bar{\varepsilon} \tag{32}$$

where $z = \begin{bmatrix} e & \eta_s \end{bmatrix}^T$, $\gamma = \min(k_1, k_s)$ and $\bar{\varepsilon} = \varepsilon + \frac{\rho_s^2}{4k_2}$.

From (26), the function $V(t)$ can be written as

$$V = \frac{1}{2} z^T \begin{bmatrix} J & 0 \\ 0 & L_s \end{bmatrix} z \tag{33}$$

and can thus be bounded using the Raleigh inequality as

$$\lambda_{\min} \|z\|^2 \le V \le \lambda_{\max} \|z\|^2 \tag{34}$$

where $\lambda_{\min} = \frac{1}{2}\min(J, L_s)$ and $\lambda_{\max} = \frac{1}{2}\max(J, L_s)$.

From (32) and (34), the following relationship is obtained

$$\dot{V} \le -\frac{\gamma V}{\lambda_{\max}} + \bar{\varepsilon} \tag{35}$$

From (34) and (35), the term $\|z(t)\|$ can be upper bound as

$$\|z(t)\| \le \sqrt{\beta_0 \exp(-\beta_1 t) + \beta_2\left[1 - \exp(-\beta_1 t)\right]} \tag{36}$$

where $\beta_0 \triangleq \frac{\lambda_{\max}}{\lambda_{\min}} \|z(t_0)\|^2$, $\beta_1 \triangleq \frac{\gamma}{\lambda_{\max}}$, and $\beta_2 \triangleq \frac{\lambda_{\max}\bar{\varepsilon}}{\lambda_{\min}\gamma}$.

From (36), it can be shown that $e(t), \eta_s(t) \in \mathcal{L}_\infty$. Similarly, (7) and Remark 3, allow for $\omega(t) \in \mathcal{L}_\infty$. From Assumption 7, it is apparent that $f(\cdot) \in \mathcal{L}_\infty$. It can be shown from (10) that $I_d(t) \in \mathcal{L}_\infty$. From (7), it can be concluded that $I_s \in \mathcal{L}_\infty$. From (8) and Remark 2, it can be shown that $\dot{\omega}, \dot{e} \in \mathcal{L}_\infty$. After taking the time derivative of (10), $\dot{I}_d(t) \in \mathcal{L}_\infty$ using Remarks 3 and 4. From (11), it can be shown that $v_s(t) \in \mathcal{L}_\infty$. The application of standard signal chasing arguments permits the conclusion that all signals in the closed-loop system remain bounded. In particular, from (7) and (9), it can be implied that $\dot{\eta}_s(t) \in \mathcal{L}_\infty$. Using Assumption 7, it is clear that $\dot{f}(\cdot) \in \mathcal{L}_\infty$. After taking the time derivative of (7), it can be shown that $\dot{I}_s(t) \in \mathcal{L}_\infty$. After taking the time derivative of (5), it is apparent that $\ddot{\omega}(t) \in \mathcal{L}_\infty$. Finally it may be concluded that $\ddot{f}(\cdot) \in \mathcal{L}_\infty$ using Assumption 7.

B. *Simulation parameters*

Table I lists the parameter values used in the numerical simulation of Section VII.

TABLE I
SIMULATION PARAMETERS AND VALUES

Parameters	Value	Units
A	7.07	m^2
B	1.151	$kg.m^2/s$
I_r	3	A
k	5000	-
k_f	500	-
k_s	100	-
K_B	0.352	-
L_s	60	H
M	500	$kg.m^2$
N	10	-
R	1.5	m
R_s	60	Ω
v	3	$m.s^2$
Rated V_s	240	V
β	0.2	deg
Δ	500	-
ε	0.1	-
ρ	1.2	kg/m^3